Advances in Science and Technology Research Journal

Advances in Science and Technology Research Journal, 2026, 20(6), 93–106
https://doi.org/10.12913/22998624/216767
ISSN 2299-8624, License CC-BY 4.0

Received: 2025.11.28
Accepted: 2026.04.15
Published: 2026.05.01

Modeling of the front wing cross-section for a formula student vehicle

Adam Piszczatowski[1], Małgorzata Kmiotek[2*], Adrian Kordos[2], Adam Zaremba[1]

[1] Graduate Student from Faculty of Mechanical Engineering and Aeronautics Rzeszow University of Technology, Al. Powstańców Warszawy 12, 35-029 Rzeszów, Poland
[2] Department of Aerospace Engineering, Faculty of Mechanical Engineering and Aeronautics Rzeszow University of Technology, Al. Powstańców Warszawy 12, 35-029 Rzeszów, Poland
* Corresponding author's e-mail: kmimal@prz.edu.pl

ABSTRACT

The aim of this article was to design an optimal cross-section of the front wing for a Formula Student vehicle, conducted in compliance with applicable technical and aerodynamic regulations. The article focuses on analyzing various configurations of four-element wings supported by computational fluid dynamics (CFD) simulations to evaluate multiple wing configurations and to study their aerodynamic properties. Key design variables included angle of attack, geometry, and chord length ratio on aerodynamic efficiency. Numerical analyses were performed using the finite volume method in ANSYS Fluent, and aerodynamic performance was assessed based on downforce and drag coefficients, which are crucial for the vehicle's performance. The optimization criterion was defined as the maximization of the product of wing chord length and downforce coefficient $c \cdot c_z$, enabling a balanced assessment of aerodynamic efficiency. Among ten analyzed configurations, the optimal design achieved a maximum value $c \cdot c_z$ of 1.010 m, with a downforce coefficient of c_z =2.056 and a drag coefficient of c_x= 0.249. The optimal configuration angles of attack of -7°, 7.5°, 28°, And 38°, along with chord length ratios of 0.73, 0.53, and 0.39. The results confirm that CFD-based parametric optimization is an effective approach for enhancing front wing aerodynamic efficiency in Formula Student applications.

Keywords: formula student, front wing, aerodynamic optimization, computational fluid dynamics (CFD), downforce.

INTRODUCTION

The design of front wings in Formula 1 racing cars plays a crucial role in vehicle aerodynamics. Since the beginnings of Formula 1 in the early 1950s, aerodynamics has undergone significant evolution, from minimizing air resistance to focusing on aerodynamic downforce (1–4).

The origins of formula racing cars date back to times when vehicles served mainly for personal transport, and over time, they began to evolve towards sport and entertainment. The first formula cars were designed to achieve high maximum speeds, with the primary goal of reducing air resistance. However, at high speeds, vehicles developed lift forces, affecting their stability. To improve their handling and stability, engineers installed inverted wing profiles, generating negative lift, known as downforce (4, 5).

The importance of aerodynamic downforce for a race car's performance is enormous, as it allows for an increase in lateral and tangential tire forces, influencing faster cornering as well as better acceleration and braking. The balance of downforce between the front and rear wheels is crucial for the vehicle's equilibrium and efficiency (6–8).

The first use of wings in formula racing appeared in 1966, when Jim Hall equipped his Chaparral 2E with a rear spoiler. In 1967, the Chaparral 2F became the first racing car to use a wing to increase downforce, which improved driving stability and handling (9). Since then, the use of wings in racing cars has rapidly developed.

The front wing, generating a significant portion of the race car's downforce, has evolved from simple, single-element constructions, e.g., in the Lotus 49 car, to advanced multi-element wings used in the 2010s, thanks to the development of computational fluid dynamics (CFD) methods. In the 1970s and 1980s, wings in Formula 1 evolved, introducing complex geometry and multi-element constructions, which allowed for better utilization of the ground effect – a phenomenon where airflow under the wing in close proximity to the ground is accelerated, increasing aerodynamic downforce – and an increase in aerodynamic efficiency(1, 3, 10–15).

New Formula 1 technical regulations for 2023 introduced changes in the aerodynamic concept of race cars, reducing the aerodynamic efficiency of wings, but still maintaining them as a key design element. Aerodynamic analyses of wings in Formula 1 include aerodynamic interactions between the wing and wheels, as well as optimization of the entire race car (7, 16–22).

Experiences from Formula 1, such as multi-element wings and ground effect, inspired the design of the wing for the Formula Student vehicle. Although Formula 1 regulations are more restrictive, the aerodynamic principles are similar, and the design of multi-element wings in Formula Student uses the same concepts, adapted to the specifics of student competitions (23–29).

During the design of the front wing for the Formula Student vehicle for 2024 (30), the priority was to comply with the series regulations, while also referring to the technical guidelines of Formula 1 (9). For this purpose, a uniform wing cross-section was chosen, which meets all Formula Student criteria regarding dimensions, placement, strength, and aerodynamics. The design also took into account Formula 1 regulations, which limit the number of closed wing sections to four, and accordingly, the maximum allowed number of sections was used. Thanks to this, the wing corresponds to the latest standards in motorsport and ensures simplicity in construction. Maintaining a uniform wing cross-section along its entire length is necessary to ensure compliance with Formula Student regulations and simplifies CFD modelling. A constant 2D cross-section facilitates avoidance of features disallowed by the FIA, such as specific curvature radii, which would be more difficult to achieve in designs with multiple cross-section profiles. The main goal of the work was to design a four-element wing for a Formula Student vehicle that provides maximum aerodynamic efficiency, characterized by maximum downforce with minimum aerodynamic drag.

PROBLEM STATEMENT

The design of the front wing for a Formula Student vehicle is based on the application of the Formula Student Germany 2024 regulations, which precisely define the required dimensions and placement of aerodynamic elements of the vehicle (30). In particular, the regulations define two areas for the placement of aerodynamic devices: area A, where aerodynamic devices can reach up to 500 mm above the ground, and area B, where devices must be lower than 250 mm above the ground, especially in the front part of the vehicle, to ensure safety and compliance with regulations. According to the regulations, the wing must be located at least 75 mm from the front wheel, but cannot extend beyond 700 mm from it. The height of the wing is also limited depending on the area: a maximum of 250 mm in area B and up to 500 mm in area A (Figure 1).

Area B was chosen as the limiting design dimension because it imposes more restrictive constraints (maximum height 250 mm), which necessitates precise design to maximize downforce within these limitations. This choice stems from the fact that in Formula Student, where tracks are characterized by many turns, downforce is crucial for improving grip, and the limitations of area B force a more effective use of the available space.

It is crucial to design the wing so that it maintains its effectiveness during cornering at a typical speed of 15 m/s, which corresponds to a Reynolds number in the range of approximately $Re = 5 \cdot 10^5$, focusing on generating maximum downforce with minimization of aerodynamic drag as a secondary factor. The ground effect, which enhances downforce, is a key parameter here, depending on the height of the wing relative to the ground. Utilizing the maximum permissible heights within the regulations can bring benefits, but maintaining a uniform wing cross-section along its entire length is necessary to ensure compliance with Formula Student regulations.

When designing the wing with area B as the limiting design dimension, it is important to use slots to achieve the desired aerodynamic properties at high camber and angle of attack. The

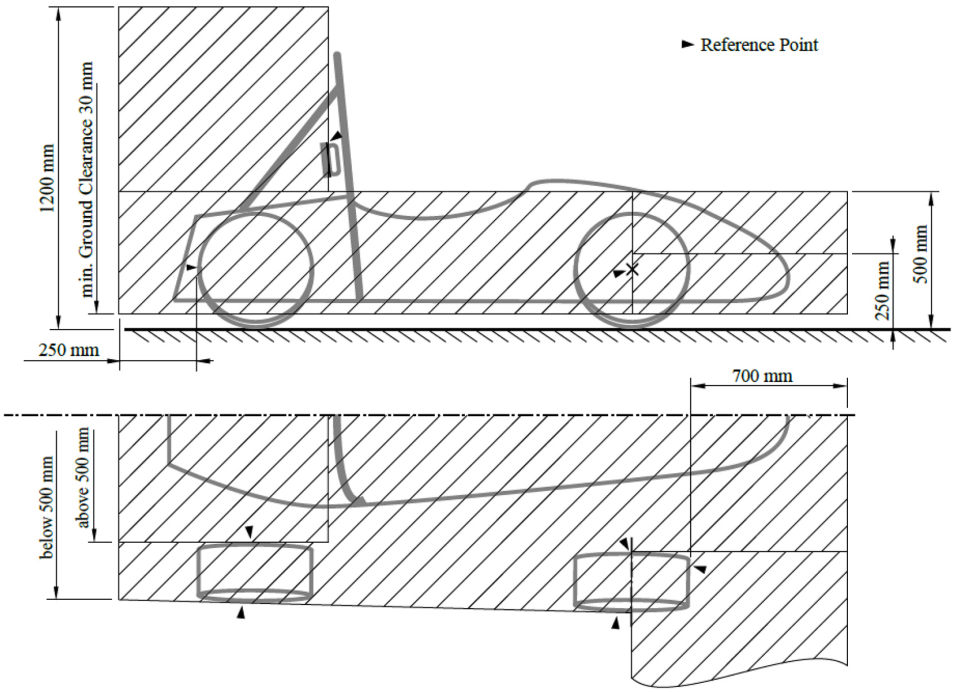

Figure 1. Permissible areas for the front wing according to the Formula Student Germany 2024 regulations (30). Area A: maximum height 500 mm, area B: maximum height 250 mm

multi-element construction of such a wing allows for stable airflow and avoidance of flow separation at the rear of the wing, which is crucial for maintaining continuous downforce generation.

The design of the front wing cross-section for a Formula Student vehicle is a complex task that requires consideration of both competition regulations and advanced aerodynamic principles.

A wing consisting of four elements was analyzed, with the first element being an Eppler E407 airfoil, and for the next three, a Selig S1223 airfoil was chosen. The choice of the Eppler E407 airfoil for the main wing element results from its aerodynamic properties (Figure 2), which are optimal when ground effect is present, especially due to its ability to generate stable lift at low speeds and low Reynolds numbers. This airfoil is characterized by a flat rear surface, which promotes a favorable pressure gradient and ensures stable airflow in the wing slot region. This, in turn, is crucial for maintaining continuous airflow, especially in conditions close to the surface. The applied airfoil thus ensures aerodynamic efficiency while limiting the risk of airflow separation (31).

The use of the Selig S1223 airfoil is justified by its ability to generate a high lift coefficient at low Reynolds numbers (Figure 2), which is particularly advantageous in ground effect conditions. This airfoil, due to its large camber (8.1%) and maximum lift coefficient, is optimal for use in places where maximization of downforce is required, especially at low speeds typical of Formula Student vehicle operation (32).

The use of a larger ground clearance of 50 mm compared to the minimum value of 30 mm specified in the regulations aims to account for dynamic changes in the vehicle's position during maneuvers such as braking or cornering, which is important for maintaining continuous aerodynamic downforce.

In the wing design, the selection criterion was based on maximizing the product of the downforce coefficient and the resultant wing chord, denoted as $c \cdot c_z$, taking into account the drag coefficient and the resultant wing chord, denoted as $c \cdot c_X$. The choice of this parameter stems from the fact that in Formula Student, where tracks are characterized by many turns and short straights, the priority is to maximize downforce for better grip in corners, and aerodynamic drag is secondary, as long as it does not significantly affect maximum speed. The product $c \cdot c_z$ considers both the downforce and the physical size of the wing, which is important in the context of regulatory and design constraints. The final choice of the cross-section is therefore the result of a careful balance between maximizing downforce and design and regulatory limitations.

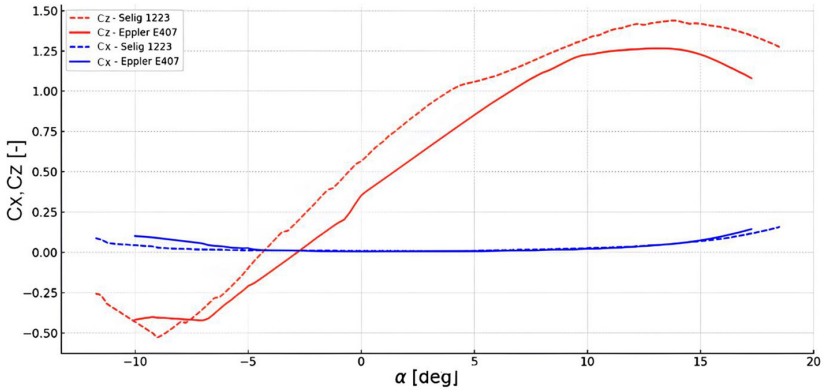

Figure 2. Aerodynamic characteristics of S1223 and Eppler E407 airfoils for Reynolds number $Re = 5 \cdot 10^5$ (32)

NUMERICAL METHOD AND BOUNDARY CONDITIONS

In the design process of the front wing cross-section for the Formula Student vehicle, the Finite Volume Method (FVM) and ANSYS Fluent 2021 R1 software package were used to solve the equations describing the flow. This approach is based on the principles of mass and momentum conservation in incompressible fluid flows, expressed by the following equations (33):

$$\frac{\partial \rho}{\partial t} + div(\rho V) = 0 \tag{1}$$

$$\rho \frac{\partial V}{\partial t} = \rho F - \nabla p + \mu \Delta V \tag{2}$$

where: p is the fluid density [kg/m^3], V is the fluid velocity vector [m/s], F is the vector of body forces acting on the fluid [N], p is the pressure [Pa], μ is the dynamic viscosity coefficient [Pa·s].

Equations 1–2 represent the general conservation of mass and momentum, which are solved by ANSYS Fluent within the computational domain surrounding the wing cross-section. After applying problem-specific assumptions, simplifications resulting from the geometry are steady-state, incompressible, two-dimensional flow and negligible body forces – the equations reduce to Equations 3–5:

- Continuity equation:

$$\frac{\partial u_x}{\partial x} + \frac{\partial u_y}{\partial y} = 0 \tag{3}$$

- Momentum equation (Navier-Stokes):

$$\rho\left(u_x \frac{\partial u_x}{\partial x} + u_y \frac{\partial u_x}{\partial y}\right) = -\frac{\partial p}{\partial x} + \mu\left(\frac{\partial^2 u_x}{\partial x^2} + \frac{\partial^2 u_x}{\partial y^2}\right) \tag{4}$$

$$\rho\left(u_x \frac{\partial u_y}{\partial x} + u_y \frac{\partial u_y}{\partial y}\right) = -\frac{\partial p}{\partial y} + \mu\left(\frac{\partial^2 u_y}{\partial x^2} + \frac{\partial^2 u_y}{\partial y^2}\right) \tag{5}$$

where: u_x is the fluid velocity component in the x-direction [m/s], u_y is the fluid velocity component in the y-direction [m/s].

The flow character was defined using the Reynolds number, specified as:

$$Re = \frac{\rho V c}{\mu} \tag{6}$$

where: ρ – air density [kg/m^3], V – vehicle speed [m/s], c – resultant wing chord [m], μ – dynamic viscosity of air [Pa·s].

The aerodynamic efficiency (d) of the Formula Student vehicle's front wing was defined as the ratio of the downforce coefficient to the drag coefficient and presented by the formula:

$$d = \frac{c_z}{c_x} \tag{7}$$

where: c_z is the downforce coefficient [-], c_x is the drag coefficient [-].

Boundary conditions for the computational domain include:

- "velocity inlet" for the air inlet (quarter circle, with a velocity equal to 15 m/s),

- "pressure outlet" for the outlet,
- "wall no slip" for the wing surface,
- "moving wall with no slip" for the wheel and the race track, to reflect their actual movement.

In the 2D simulation process, the Reynolds-Averaged Navier-Stokes (RANS) approach was utilized, employing the $k - \omega$ *SST* (shear stress transport) turbulence model, which combines the advantages of the $k - \omega$ model in near-wall regions and the $k - \varepsilon$ model further from the wall. The choice of the $k - \omega$ *SST* model is dictated by its ability to better predict fluid properties, especially in flow configurations associated with Formula Student vehicles (20,21,33–35).

The computational domain was designed with the detailed reproduction of flow conditions encountered by the Formula Student vehicle during driving in mind, and its configuration is presented in Figure 3. It consists of three main elements: inlet, outlet, and moving surface. The inlet, being a quarter circle, along with the upper wall and the outlet defined as the rear wall of the domain, form the boundaries through which airflow is introduced and released from the system.

An adaptive mesh was used in the calculations, where the $y+$ parameter was used to determine the height of the first mesh element, based on the flat-plate boundary layer theory (33) $y+ = 1$, dynamic viscosity $\mu = 1.79 \cdot 10^{-5}$ *Pa* · s, density ρ 1.77 *kg/m*^{3}, and Reynolds number $Re = 5 \cdot 10^{-5}$, which allowed calculating the base height of the first element $\Delta s = 2.2 \cdot 10^{-5}$ m. The maximum size of the mesh elements was 0.3 m. The validation of numerical model was performed by comparing with the experimental setup (31). The good agreement between numerical and experimental results was obtained.

The geometry of the analyzed system is presented in Figures 4a and 4b. Ten different wing configurations were considered in the studies, focusing on modifying parameters such as: mutual angles of attack of the elements (α_1, α_2, α_3, α_4), where the angle of attack of the main element (α_1) is measured relative to the ground, while the angles of the additional elements are measured relative to the chord of the preceding element, with variable chord length ratios of the elements (c_2/c_1, c_3/c_1, c_4/c_1); and constant relative slot heights between elements (g_1/c , g_2/c, g_3/c) and constant ratios of inlet length to slots (o_1/c, o_2/c, o_3/c). The geometric parameters describing the geometry of the Formula Student vehicle's front wing are presented in Table 1. In this work, the resultant chord (c) of the wing is defined as the distance measured from the nose (leading edge) of the first airfoil (Eppler E407) to the trailing edge of the last airfoil (Selig S1223). This parameter reflects the total length of the wing along its chord and depends on the arrangement of all four airfoils, their individual chord lengths ($c_1 - c_4$), and angles of attack ($\alpha_1 - \alpha_4$). This value is crucial in calculating the product $c \cdot c_z$, which serves as the selection criterion for the optimal wing configuration.

Additionally, the trailing edge length from the wheel (X_k), which remains constant for all configurations (0.21 m), significantly affects the aerodynamic space available for the wing.

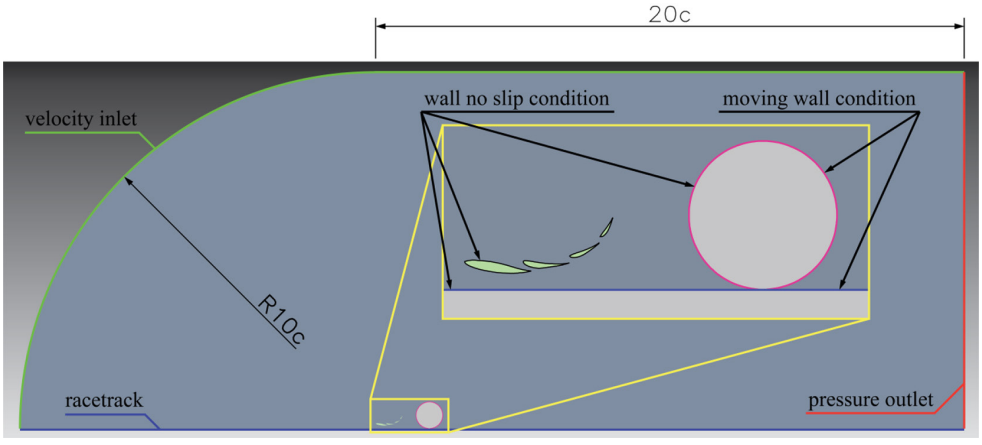

Figure 3. Computational domain with boundary conditions for CFD simulation of airflow around the front wing. Inlet: velocity inlet, outlet: pressure outlet, walls: wall no slip, moving surface: moving wall

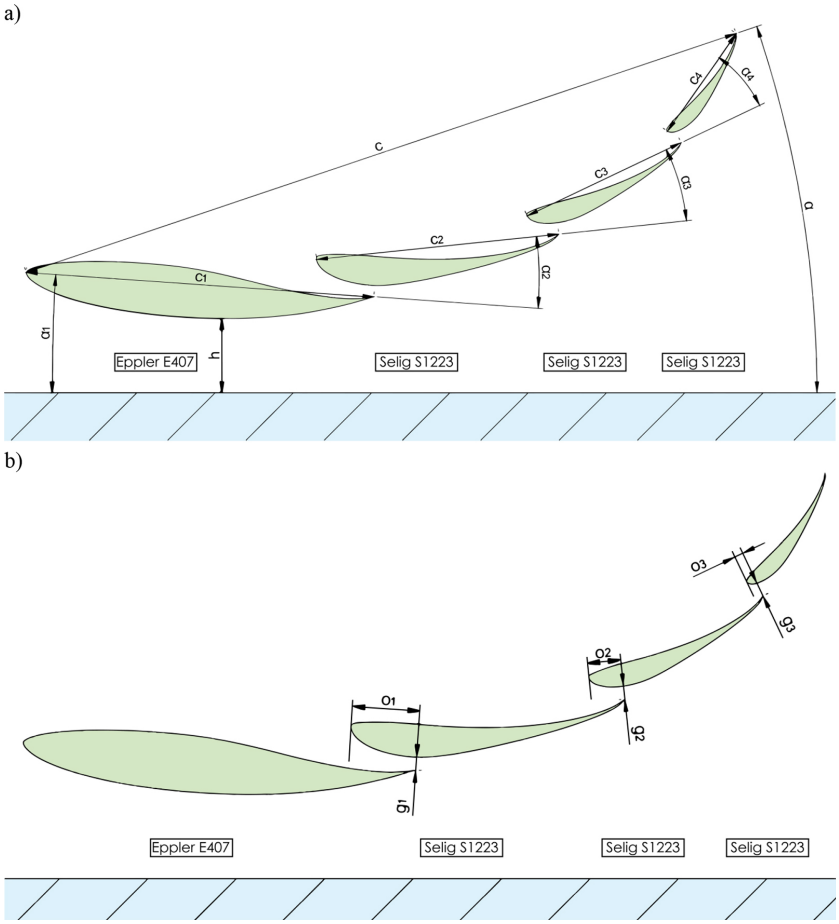

Figure 4. Geometric parameters of the front wing geometry of the slots in the front wing a) angles of attack (α_1–α_4), chord lengths of individual profiles (c_1–c_4), ground clearance (h), and resultant chord (c), measured from the nose of the first profile (Eppler E407) to the trailing edge of the last profile (Selig S1223); and resultant angle of attack (α), defined as the angle between the resultant chord and the ground b) slot heights ($g_1 - g_3$) and inlet lengths ($o_1 - o_3$)

This is essential for defining the flow around the wing and its interaction with the wheel, which can generate turbulence and affect overall efficiency.

In the study, constant values of relative slot heights (g_1/c = 1.5, g_2/c = 1.5, g_3/c = 1.5) and ratios of inlet lengths to slots (o_2/c = 8, o_2/c = 4, o_3/c = 1) were adopted, which were established based on preliminary analyses and were not subjected to optimization. The iterative process focused on selecting the angles of attack (α_1 – α_4) and chord length ratios (c_2/c_1, c_3/c_1, c_4/c_1) to maximize the product $c \cdot c_z$. These parameters were chosen discretely, and their selection was based on empirical observations regarding the product $c \cdot c_z$, which served as an indicator of aerodynamic efficiency. Geometries that led to noticeable boundary layer separation were rejected, which was a key element in the process of selecting optimal configurations.

RESULTS

The calculation results, in the form of determined aerodynamic force coefficients for individual front wing setting variants, have been presented as aerodynamic characteristics. Figure 5 shows the relationship between the product of the downforce coefficient and the resultant wing chord ($c \cdot c_z$) and the product of the drag coefficient and the resultant wing chord ($c \cdot c_z$) for 10 wing configurations. Configurations 1 and 9, representing the lowest and highest $c \cdot c_z$ product respectively, were selected for detailed analysis to examine extreme cases of aerodynamic efficiency.

According to the calculation results presented in Figure 5, it is evident that Configuration No. 1, whose parameters c_z and c are 1.519 and 0.504 respectively, yields a product $c \cdot c_z$ equal to 0.766 m. With angles of attack α_1 = -5°, α_2 = 13°, α_3 = 24.5°, α_4 = 39.5° and chord length ratios c_2/c_1 =

Table 1. Geometric parameters of the front wing for the Formula Student vehicle

Conf. No.	α_1 [°]	α_2 [°]	α_3 [°]	α_4 [°]	c_2/c_1 [-]	c_3/c_1 [-]	c_4/c_1 [-]	g_1/c [-]	g_2/c [-]	g_3/c [-]	o_1/c [-]	o_2/c [-]	o_3/c [-]	x_k [m]	c [m]
1	-5	13	24.5	39.5	0.6	0.36	0.22	1.5	1.5	1.5	8	4	1	0.21	0.504
2	-6	11.5	23.5	35	0.67	0.44	0.3	1.5	1.5	1.5	8	4	1	0.21	0.504
3	-7	12	24.5	34.5	0.67	0.44	0.3	1.5	1.5	1.5	8	4	1	0.21	0.503
4	-8	12.5	25.5	38	0.67	0.44	0.3	1.5	1.5	1.5	8	4	1	0.21	0.502
5	-7	10	27	40.5	0.67	0.44	0.3	1.5	1.5	1.5	8	4	1	0.21	0.504
6	-7	9.5	25.5	38	0.7	0.49	0.34	1.5	1.5	1.5	8	4	1	0.21	0.504
7	-7	7	27	36	0.73	0.53	0.39	1.5	1.5	1.5	8	4	1	0.21	0.505
8	-7	7.5	29	38.5	0.7	0.49	0.34	1.5	1.5	1.5	8	4	1	0.21	0.504
9	-7	7.5	28.5	38	0.73	0.53	0.39	1.5	1.5	1.5	8	4	1	0.21	0.486
10	-7	7.5	29	38.5	0.73	0.53	0.39	1.5	1.5	1.5	8	4	1	0.21	0.477

0.6, c_3/c_1 = 0.36, c_4/c_1 = 0.22. Such an approach may be aimed at stability and control, especially on racetrack corners at lower speeds, where excessive downforce may not be necessary or even desirable.

In contrast, configuration number 9 achieves the highest value of the product $c \cdot c_z$ equal to 1.010 m, with parameters c_z and c being 2.079 and 0.486 respectively. The angles of attack for this configuration are α_1 = -7°, α_2 = 7.5°, α_3 = 28.5°, α_4 = 38°, which indicates a more aggressive approach to wing design. The chord length proportions for this configuration, c_2/c_1 = 0.73, c_3/c_1 = 0.53, c_4/c_1 = 0.39, suggest the use of shorter elements in the rear part of the wing relative to the main element, which may contribute to better airflow management and increased aerodynamic efficiency. These numerical values are crucial as they indicate a potential relationship between chord length and aerodynamic efficiency.

According to the calculation results presented in Figure 5, it is evident that configuration 9 not only achieves a higher value of the product $c \cdot c_z$ but also has a higher drag coefficient value (c_x), which is 0.249 compared to 0.188 in configuration 1. This may indicate that higher aerodynamic efficiency is achieved at the cost of increased drag. However, in races such as Formula Student, where tracks are characterized by many turns and lower average speeds, downforce is a priority, and higher drag is acceptable as long as it does not significantly affect performance on straight sections.

As shown in Figure 5, configuration 9 achieves $c \cdot c_z$ = 1.010 m at $c \cdot c_x$ = 0.121 m, which is the highest result among all configurations,

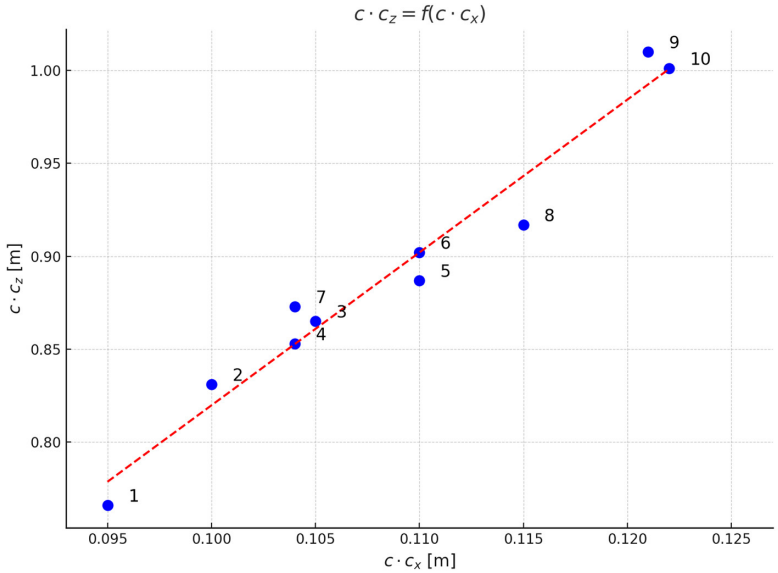

Figure 5. Relationship between the product of the downforce coefficient and resultant chord ($c \cdot c_z$) and the product of the drag coefficient and resultant chord ($c \cdot c_z$) for 10 wing configurations

while configuration 1 has $c \cdot c_z = 0.766$ m and $c \cdot c_x = 0.095$ m.

Geometric parameters of the wing, such as angles of attack α_1 to α_4, and chord ratios c_2/c_1, c_3/c_1, c_4/c_1, are crucial in aerodynamic design. For example, configuration 9 with larger chord ratios for the rear elements indicates that a larger surface area of the elements was used to increase lift force. This is a strategic approach that can significantly affect airflow behavior around the wing, reducing the risk of turbulence and airflow separation at higher speeds.

Figure 6 presents the relationship between the product of the downforce coefficient and the resultant wing chord ($c \cdot c_z$) and aerodynamic efficiency. According to the calculation results for configuration 1, $d = 8.080$ and $c \cdot c_z = 0.766$ m, we observe lower values of the $c \cdot c_z$ product, which may indicate a wing configuration that favors lower drag at the expense of downforce. Such characteristics may be preferred in situations where maintaining vehicle stability is more important than maximum grip, for example, on technical sections of the track where frequent changes of direction are more critical than maximum speeds.

Configuration 9, where $d = 8.349$ and $c \cdot c_z = 1.010$ m, stands out with an exceptionally high value of the $c \cdot c_z$ product, indicating an aggressive wing setup. The high value of aerodynamic efficiency d shows that this configuration provides strong downforce with relatively low drag, which is crucial for maintaining high grip, especially at higher speeds.

In turn, Figure 6 indicates that the aerodynamic efficiency $d = 8.349$ in configuration 9 is only slightly higher than $d = 8.080$ in configuration 1, suggesting that the increase in downforce is associated with a proportional increase in drag.

Configuration 5, where aerodynamic efficiency $d = 8.032$ and $c \cdot c_z = 0.887$ m, represents a configuration where the ratio of downforce to drag is balanced. This suggests that the wing design has been optimized to ensure good aerodynamic performance on both straight sections and in corners.

Configuration 6, with $d = 8.206$ and $c \cdot c_z = 0.902$ m, may indicate subtle improvements in wing geometry that contribute to an increase in downforce while maintaining controlled aerodynamic drag.

The lowest value of d, for configuration 8 ($d = 7.943$), with a relatively high value of $c \cdot c_z = 0.917$ m, may mean that an optimal balance between downforce and aerodynamic drag has been achieved, which is particularly important for vehicle performance.

When comparing the calculation results from Figure 6 in the context of aerodynamic efficiency, we notice that higher values of d are associated with higher values of the $c \cdot c_z$ product. This may indicate that downforce has been effectively increased with a simultaneous moderate increase in aerodynamic drag. The d values in the figure do not form a straight line, indicating that aerodynamic efficiency does not increase proportionally to downforce, and these relationships are more complex and ambiguous.

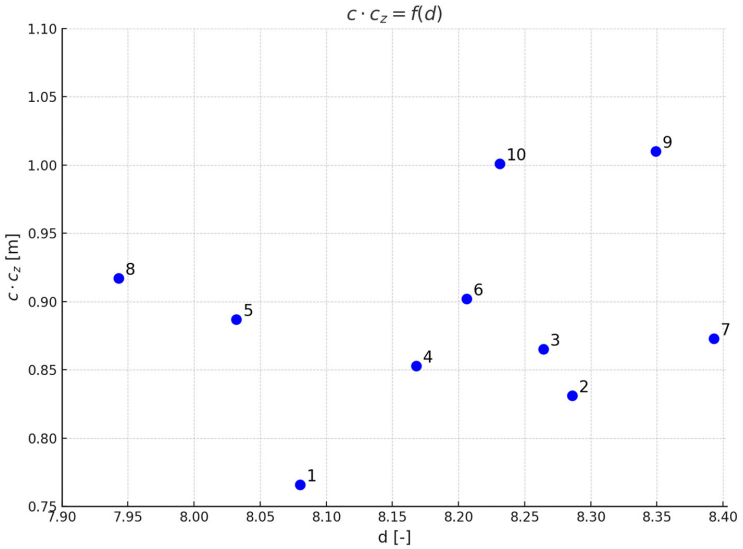

Figure 6. Influence of aerodynamic efficiency (d) on the product of the downforce coefficient and resultant chord ($c \cdot c_z$) for the analyzed configurations

In the practice of designing Formula Student vehicle wings, high values of aerodynamic efficiency d may not always mean better vehicle performance. What is most important is finding the optimal point where downforce is sufficiently high to maintain grip, but aerodynamic drag is not so large as to significantly affect vehicle performance, especially on straight sections of the track.

Analysis of the calculation results presented in Figure 7 and 8 is important in understanding the impact of the angle of attack (α) on the aerodynamics of the Formula Student vehicle's front wing. Figure 7 shows the dependence of the downforce coefficient (c_z) on the resultant angle of attack (α), defined as the angle between the resultant chord and the ground, in the range of angles of attack 17–20°, and Figure 8 presents the product of this coefficient and the wing chord length ($c \cdot c_z$) in the range of angles 17–20°. Together, they shed light on the optimization of angles of attack for achieving desired aerodynamic characteristics.

Figure 7 shows the range of angles of attack from 17.0765° to 19.127° for the respective configurations. For configuration 1, where the angle of attack is 17.7489°, the downforce coefficient c_z is equal to 1.519. This is a lower value, which in the context of racing may indicate a configuration focused on reducing drag, crucial for achieving higher speeds on straight sections of the track and in situations where excessive downforce may not be beneficial.

In contrast, configuration 10, characterized by the highest angle of attack of 19.127° and a c_z coefficient of 2.099, generates much greater downforce. Such c_z values are desirable on long, straight sections of the track, where grip is essential for achieving fast lap times.

Configuration 9, with an angle of attack of 18.9246° and one of the highest downforce coefficients c_z at 2.079, shows the potential benefits of increasing the angle of attack. This is particularly important in the context of multi-element wings, where each wing element can be optimized for different operating conditions.

From Figure 7, it appears that the maximum downforce coefficient c_z is achieved at $\alpha \approx 19°$, corresponding to configuration 10 (c_z = 2.099). Although configuration 10 has a higher downforce coefficient c_z = 2.099, configuration 9 with c_z = 2.079 and a smaller resultant chord c = 0.486 m achieves a higher product $c \cdot c_z$ = 1.010 m compared to 1.001 m for configuration 10. This results from a compromise between wing size and its aerodynamic efficiency, which is visible in Figures 5, 6, and 8, where configuration 9 surpasses configuration 10 in terms of $c \cdot c_z$, despite a lower c_z in Figure 7.

Figure 8 presents the relationship between the product of the downforce coefficient and the resultant wing chord and the resultant angle of attack of the wing chord. For configuration 9, the value $c \cdot c_z$ equal to 1.010 m at an angle of attack of 18.9246° shows that increasing the angle of attack above a certain level can lead to an exponential increase in downforce. Comparing the results for configurations 9 and 10 between Figures 7 and 8 reveals an inverse relationship; although configuration 10 has a higher angle of attack, this does

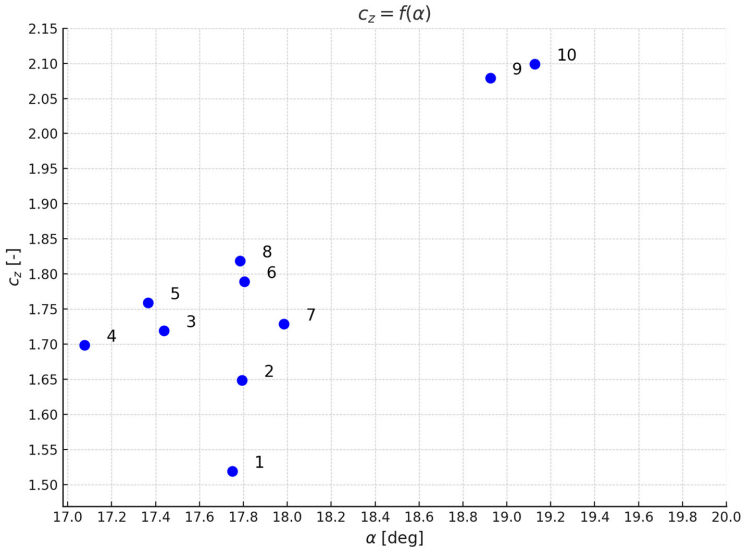

Figure 7. Dependence of the downforce coefficient (c_z) on the resultant angle of attack (α) for wing configurations in the range 17–20°

not necessarily translate to a greater value of the $c \cdot c_z$ product, suggesting that there is an optimal angle of attack for maximizing downforce.

In Figure 8, configuration 1 with an angle of attack of 17.7489° and a $c \cdot c_z$ value of 0.766 m, and configuration 10 with an angle of attack of 19.127° and a $c \cdot c_z$ value of 1.001 m, show that chord length has a significant impact on the aerodynamic efficiency of the wing. It should be remembered that the chord length (c) can vary depending on the specific wing design, which shows that the product $c \cdot c_z$ does not always increase proportionally to the angle of attack.

The middle range of angles of attack, as in configurations 5 and 6 with values of 17.3655° and 17.805° respectively, shows that even small changes in the angle of attack can affect downforce. Configuration 5 with a $c \cdot c_z$ value of 0.887 m and configuration 6 with a $c \cdot c_z$ value of 0.902 m highlight that careful adjustment of the angle of attack can lead to improved aerodynamic characteristics without significantly increasing this angle.

Configurations 5 and 6, with $c \cdot c_z$ products close to 0.9 m, are particularly interesting. They show that subtle optimization of the angle of attack can lead to improved aerodynamic performance of the wing without a significant increase in the angle of attack. This indicates the possibility of achieving high downforce with a moderate increase in aerodynamic drag.

To visualize the flows around the front wing of the vehicle, velocity distributions and streamlines for configuration No. 1 and configuration No. 9 are shown in Figures 9 and 10. According to the calculation results shown in Figure 9, for configuration 1, flow separation occurred on the lower leading edge of the fourth element, which is an undesirable phenomenon from an aerodynamic point of view, as it causes a loss of the desired suction under the wing. Flow separation is a phenomenon in which the airflow detaches from the wing surface, creating vortices, which leads to a reduction in downforce and an increase in aerodynamic drag. The research results also show for configuration 1 limited use of the third element in generating downforce, which is visible in the slowing of airflow on its lower edge.

In contrast, the research results for configuration 9 (Figure 10) show a much more effective configuration. Higher air velocity values around the wing were achieved, which contributed to increased suction, especially on the lower surface of elements 1, 2, and 3. The fourth element, despite flow separation occurring at the leading edge, does not contribute to a significant reduction in aerodynamic efficiency thanks to modifications in geometry and optimization of the slots between the elements. In this configuration, precise angles of attack and appropriately designed slots were used, which allowed for effective airflow management, limiting the negative effects of separation and turbulence.

Key differences between the calculation results of configurations 1 and 9 can also be observed in the range of maximum flow velocity. Configuration 9 achieves a velocity of up to 27.19

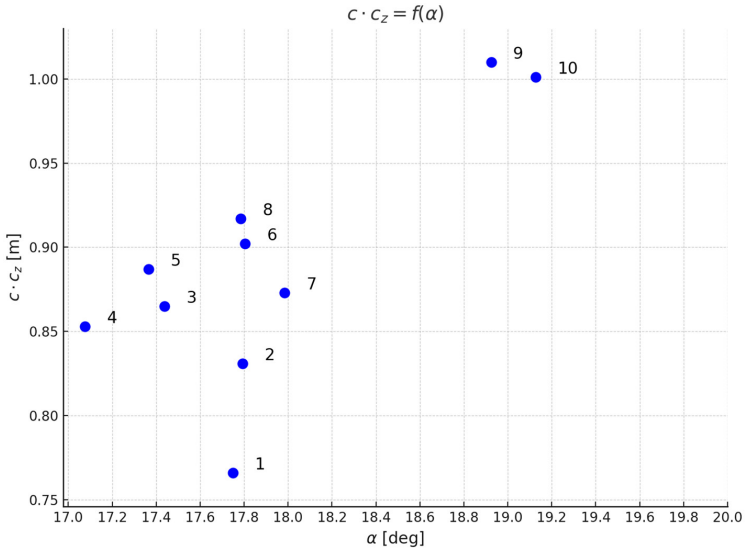

Figure 8. Dependence of the product $c \cdot c_z$ on the resultant angle of attack (α) for the analyzed wing configurations

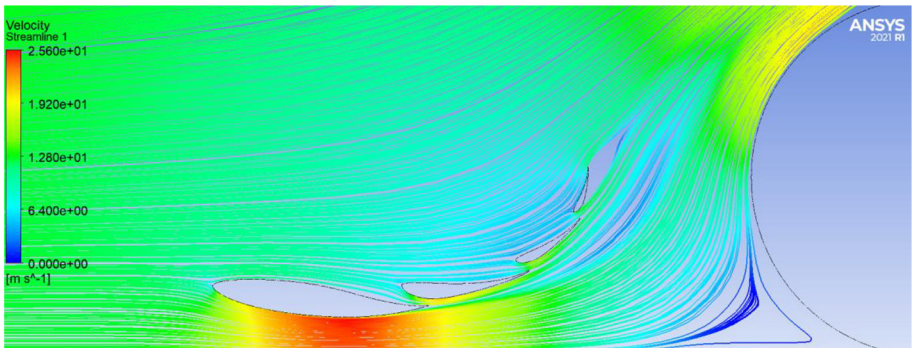

Figure 9. Air velocity distribution and streamlines for configuration 1

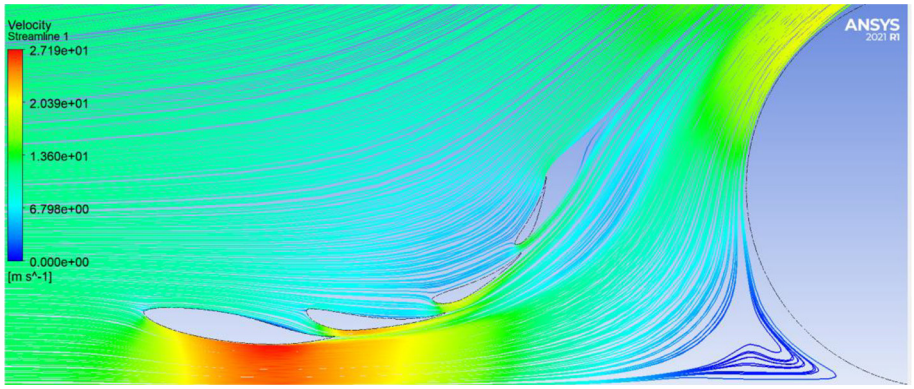

Figure 10. Air velocity distribution and streamlines for configuration 9

m/s, which indicates greater aerodynamic efficiency compared to the calculation results of configuration 1, where the velocity does not exceed 25.6 m/s. The higher flow velocity in configuration 9 translates into better aerodynamic properties, as higher air velocity on the lower surface of the wing results in greater suction and downforce.

The pressure distribution along the front wing cross-section is shown in Figures 11 and 12 for the respective geometries of the wing model from configurations 1 and 9. Based on the calculation results presented in Figure 11 for configuration 1, it can be observed that the pressure distribution along the wing does not generate optimal suction, especially in the area of the third element. This phenomenon, likely resulting from insufficient acceleration of airflow over the element, leads to insufficient downforce and destabilization of the vehicle on the track. This is a clear signal that the angle of attack or the slots between the elements require correction to improve grip and overall aerodynamic performance.

According to the calculation results presented in Figure 12, significantly higher suction values on the lower edge of elements 1, 2, and partially 3 indicate more effective airflow acceleration and better

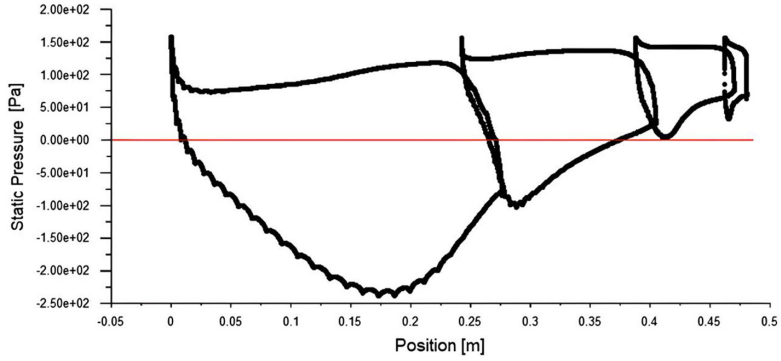

Figure 11. Static pressure distribution on the wing for configuration 1

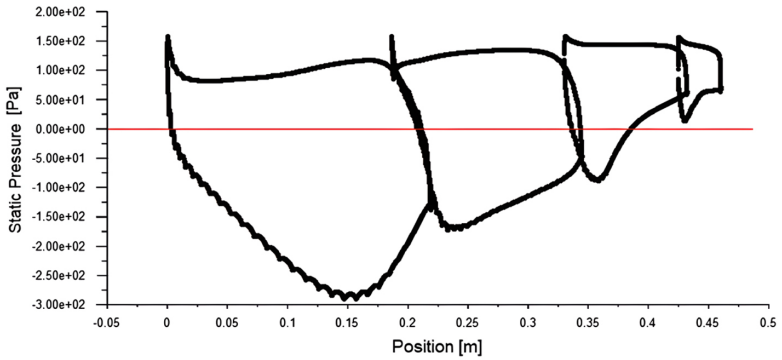

Figure 12. Static pressure distribution on the wing for configuration 9

utilization of aerodynamic principles for generating downforce. Although the fourth element also experiences flow separation, appropriate corrections in the wing geometry minimize the negative impact of this phenomenon, allowing for the maintenance of desired aerodynamic properties.

In the analysis of static pressure values, the calculation results for configuration 9 show higher values compared to configuration 1. On the first element of configuration 9, a suction value of -300 Pa was observed, exceeding the -250 Pa from configuration 1. According to aerodynamic principles, higher suction values indicate faster airflow and increased downforce. Additionally, the second element in configuration 9 generates a suction of -175 Pa, which is also higher than the -100 Pa from configuration 1, confirming the greater aerodynamic efficiency of configuration 9.

CONCLUSIONS

The main goal of the work was to design a four-element wing for a Formula Student vehicle that ensures maximum aerodynamic efficiency, characterized by maximum downforce with minimum aerodynamic drag.

The design of the front wing for the Formula Student vehicle considered the application of the Formula Student Germany 2024 regulations, which precisely define the required dimensions and placement of the vehicle's aerodynamic elements, while also referring to the technical guidelines of Formula 1.

For this purpose, a uniform wing cross-section was chosen, which meets all criteria of the Formula Student regulations and Formula 1 regulations, limiting the number of closed wing sections to four. A constant 2D cross-section facilitates the avoidance of features disallowed by the FIA, such as specific curvature radii.

Numerical studies using the finite volume method and Ansys Fluent software were performed for ten different wing configurations, focusing on modifying variables such as: mutual angles of attack of the elements, proportions of element chord lengths, relative heights of slots between elements, and the length of the inlet to the slots.

During the research, an iterative approach was used to define the chord of the complete wing, with the intention of maximally utilizing the available construction space, while maintaining optimal aerodynamic proportions for a given set of parameters. Based on the obtained research results in the form of aerodynamic force coefficients, pressure distributions, and velocities, two extreme wing configurations were selected for further analysis, representing the lowest and highest product of the coefficient c_z and chord c, i.e., configuration No. 1 and configuration No. 9. The work analyzed the results in the form of relationships between aerodynamic force coefficients and the geometric parameters of the wing.

Analyzing the details of the wing construction, configuration 1 seems not to utilize the full potential of the elements in generating downforce. The limited use of the third element, related to the slowing of flow on its lower edge, indicates the need for optimization of both angles of attack and slots between elements. In contrast, in configuration 9, the full utilization of elements 1, 2, and 3 in the process of generating downforce shows the effectiveness of the wing design. However, it should be noted that in both configurations, flow separation occurs on the fourth element, which indicates a common challenge in designing Formula Student vehicle wings and the need for further research in this area.

In configuration number 9 for the Formula Student vehicle, controlled slowing of airflow on the upper trailing edge of the first and second elements is a desirable phenomenon, as it contributes to increasing the wing's downforce. This is important for improving the vehicle's grip and stability on the track. In contrast, in configuration number 1, the absence of stagnation in these same areas indicates potentially weaker aerodynamic downforce properties, which may negatively affect the overall performance of the vehicle during races.

The conducted research showed that configuration number 9 achieved the highest level of aerodynamic efficiency among all ten analyzed configurations. This result was achieved thanks to an optimal combination of various aerodynamic parameters, such as angle of attack, wing geometry, and the ratio of the wing chord length to the sum of the lengths of all elements. Configuration 9 demonstrated that appropriate adjustment of each of these elements is crucial for achieving optimal aerodynamic characteristics.

In particular, the analysis showed that configuration 9 was characterized not only by the highest $c \cdot c_z$ product but also by an exceptional ability to generate significant downforce with a simultaneous moderate increase in aerodynamic drag. Such a balance is essential in Formula Student races, where both grip and minimization of drag are key to the vehicle's speed and maneuverability. This configuration proved that the aerodynamic efficiency of the wing can be maximized not only by increasing its size but primarily through intelligent shaping and positioning of each wing element, which enables more effective airflow management.

Additionally, detailed airflow studies in configuration number 9 showed that the proper configuration and calibration of the angles of attack of each wing element, as well as the optimal spacing of the elements relative to each other, had a decisive impact on the overall aerodynamic performance. Optimization of the angles of attack was crucial, especially for elements located closer to the wing's leading edge, where initial downforce is generated. Configuration 9 showed that even small changes in these angles can significantly affect airflow characteristics and downforce, confirming that precise calibration of each element is necessary to achieve maximum aerodynamic efficiency.

Consequently, configuration 9 provided convincing evidence that the appropriate application of aerodynamic principles, combined with advanced computational methods, can lead to significant improvements in the aerodynamic performance of a Formula Student vehicle's front wing. These results underscore the importance of a holistic approach to wing design, where every aspect, from the shape and size of the elements, through their mutual arrangement, to the detailed optimization of angles of attack, must be carefully considered and synchronized to achieve optimal performance.

The research showed that optimal angles of attack in the range $\alpha_1 = -7°$, $\alpha_2 = 7.5°$, $\alpha_3 = 28.5°$, $\alpha_4 = 38°$ and chord proportions $c_2/c_1 \approx 0.73$, $c_3/c_1 \approx 0.53$, $c_4/c_1 \approx 0.39$ allowfor achieving high downforce with acceptable aerodynamic drag.

The analysis showed that configuration 9 is optimal due to the highest product $c \cdot c_z = 1.010$ m (Fig. 5), achieved with angles of attack $\alpha_1 = -7°$, $\alpha_2 = 7.5°$, $\alpha_3 = 28.5°$, $\alpha_4 = 38°$, chord proportions $c_2/c_1 = 0.73$, $c_3/c_1 = 0.53$, $c_4/c_1 = 0.39$, ground clearance $h = 50$ mm, relative slot heights $g_1/c = 1.5$, $g_2/c = 1.5$, $g_3/c = 1.5$, and ratios of in let lengths to slots $o_1/c = 8$, $o_2/c = 4$, $o_3/c = 1$. Compared to configuration 10, which has a higher downforce coefficient $c_z = 2.099$ but a lower product $c \cdot c_z = 1.001$ m, configuration 9 offers a better compromise, which is important in the context of maximizing downforce while maintaining acceptable aerodynamic drag. Configuration 9 provides higher flow velocities (27.19 m/s) and greater suction (-300 Pa), which increases downforce compared to configuration 1 ($c \cdot c_z = 0.766$ m, Figure 5). Despite higher drag ($c_x = 0.249$ vs. 0.188 in configuration 1), configuration 9 offers the best compromise for improving grip in Formula Student conditions.

REFERENCES

1. Katz J. Race Car Aerodynamics: Designing for Speed. Cambridge, MA, USA: Bentley Publishers; 1996; 280.
2. Lau CS, Srigrarom S. Flow field around the front wing of Formula One racing car model: BAR Honda 003 and MP4-21 under ground effect. Int J Aerodyn. 2010;1(1):72.
3. Seljak G. Race car aerodynamics. university of ljubljana faculty of mathematics and physics, Department of Physics; 2008.
4. Hou X. Evolution of the formula one front wing assembly. Theor Nat Sci. 2024;53(1):159–68.
5. Castro X, Rana ZA. Aerodynamic and structural design of a 2022 formula one front wing assembly. Fluids. 2020;5(4):237.
6. Tharun N, Rautwar S, Dasharath C, Siripuram A. Design and analysis on the front wing of formula one car.

In: AIP Conference Proceedings. 2024;100041.

7. Obeid S, Jha R, Ahmadi G. RANS simulations of aerodynamic performance of. Fluids. 2017;2(1).
8. Katz J. Aerodynamics of race cars. Annu Rev Fluid Mech. 2006;38(1):27–63.
9. One F, Championship W, Framework R, Car FO, Volumes R. 2023 Formula 1 Technical Regulations Contents. 2023.
10. Setlak L, Kowalik R, Lusiak T. Practical use of composite materials used in military aircraft. Materials (Basel). 2021;14(17):4812.
11. Landvogt B. Fluid-Structure Interaction of Racing Car Spoilers. In: Proceedings of the NAFEMS European Conference: Multiphysics Simulation. Copenhagen, Denmark; 2016;117–20.
12. Jackson F. Aerodynamic optimisation of Formula student vehicle using computational fluid dynamics. Fields J Huddersf student Res. 2018;4(1).
13. Mcbeath S. Competition Car Aerodynamics A Practical Handbook. Veloce; 2017.
14. Petrone, G., Hill, C., Biancolini M. Track by Track Robust Optimization of a F1 Front Wing using Adjoint Solutions and Radial Basis Functions. In: 32nd AIAA Applied Aerodynamics Conference. Atlanta, GA, USA; 2014.
15. Arrondeau, B., Saravana, A., Sabatés, A., Daniela S. Front Wing Design of a 2021 F1 Race Car. 2020.
16. Petkar RK, Kolgiri SG, Ragit SS. Study of front-body of formula-one car for aerodynamics using CFD. Int J Appl or Innov Eng Manag. 2014;3(3):353–9.
17. Heyder-Bruckner J. The Aerodynamics of an Inverted Wing and a Rotating Wheel in Ground Effect by. University of Southampton, 2021.
18. van den Berg MA. Aerodynamic interaction of an inverted wing with a rotating wheel. Southampton, UK: University of Southampton, 2007.
19. Bhatnagar UR. Formula 1 Race Car Performance Improvement by Optimization of the Aerodynamic Relationship between the Front and Rear Wings. State College, PA, USA: The Pennsylvania State University; 2014.
20. Louç R, Duarte GO, Mendes MJGC. Aerodynamic study of a drag reduction system and its actuation system for a formula student competition car. Fluids. 2022;7(9):3099.
21. Hirsch C. Numerical Computation of Internal and External Flows, Volume 2: Computational Methods for Inviscid and Viscous Flows. John Wiley & Sons, Inc.; 1991; 672.
22. He X, Wang J, Yang M, Yan C, Liu P, Letters AM, et al. Numerical Simulation of Gurney Flap on SFYT-15thick Airfoil. 2016.
23. Żuk K. The analysis of Formula Student race car's front wing aerodynamics. Mechanik. 2018; (12):1150–3.
24. Fabiś P, Leoniewski W, Czapla J, Kler K. Analysis of changes in the strength of the space frame of the Formula Student vehicle. Mot Transp. 2023;67(6):29–36.
25. Kiedrowski J, Jendro G, Kamiński A, Fabiś P. Aerodynamics package for formula student car WT-02. Sci J Silesian Univ Technol Ser Transp. 2020;109:55–60.
26. Wheatley G, Ali A. Designing an upper stage steering system for a Formula FSAE car. Sci J Silesian Univ Technol Ser Transp. 2021; 113:205–18.
27. Rangarajan K, Pushpananthan B, Anumolu L, Selvakumar K, Jayakumar SS. Numerical Study of Aerodynamic Flow and the Effects of Spoiler Wings on a Formula Student Race Car. In: SAE Technical Paper 2024-01-5247. 2025.
28. Md Madha J, Nawar A, Rahman MM, Ibn Akbar N. Study on the Aerodynamic Effects of SD7032 Aerofoil as Adjustable Front Wings of a Formula Student Car. In: Proceedings of the International Conference on Industrial Engineering and Operations Management. Michigan, USA: IEOM Society International; 2024.
29. Krbat'a M, Fekiač JJ, Kohutiar M, Malý M, Mikuš P. Design and optimization of the front wing for formula student monopost. Adv Sci Technol. 2025; 167:3–13.
30. Formula Student Rules 2024: Version 1.1. Formula Student Germany. 2024.
31. Usta O. A Numerical Study on the Aerodynamic Performance of the S1223 Airfoil in Low Reynolds Number Conditions. In: International Conference on Engineering, Natural Sciences, and Technological Developments (ICENSTED 2024). 2024; 798–804.
32. Airfoil Tools. Airfoil Tools. 2025.
33. White FM. Fluid Mechanics. 8th ed. New York, NY, USA: McGraw-Hill Education; 2016.
34. Karaki A, Abu Sirreya M, Zalloum M, Amro H. Enhancing vehicle performance through the application of airfoils as spoilers with movable trailing edge. F1000Research. 2025; 14:469.
35. Laguna-Canales AS, Urriolagoitia-Sosa G, Romero-Ángeles B, Martinez-Mondragon M, García-Laguna MA, Yparrea-Arreola RI, et al. Numerical evaluation of the effectiveness of the use of endplates in front wings in formula one cars under multiple track operating conditions. Fluids, 2024; 9(10): 232.